Creation and annihilation of conducting filaments in mesoscopic manganite structures

T. Wu* and J. F. Mitchell
Center for Nanoscale Materials, Materials Science Division, Argonne National Laboratory, 9700 South Cass Avenue, Argonne, Illinois 60439, USA

(Received 28 July 2005; revised manuscript received 15 October 2006; published 26 December 2006)

Anomalous transport properties are observed in mesoscopic (several hundreds of nanometers to several micrometers) structures of manganite $Pr_{0.65}(Ca_{0.75}Sr_{0.25})_{0.35}MnO_3$: (i) spontaneous jumps of resistance occur during both the ramping of magnetic field and the relaxation after the field cycle; and (ii) in certain ranges of temperature and magnetic field, steplike negative differential resistance (NDR) emerges in the current vs voltage measurements as the bias voltage reaches critical values. Two elements are responsible for the appearance of these giant sharp resistive steps: (i) a field- and temperature-dependent mixture of ferromagnetic metallic (FMM) and charge-ordered insulating (COI) phases found in this material; (ii) similarity between device dimensions and the size of competing FMM and COI domains. The phenomenology of the observed spontaneous steps is consistent with the filamentary conduction that has been previously observed in these materials with multiphase coexistence. The switching of individual conducting filaments manifests themselves as the discrete resistance steps in the mesoscopic samples while its effect is much less visible in continuous films. A local Joule heating-induced annihilation of conducting filaments is proposed as the underlying mechanism for the NDR.

DOI: 10.1103/PhysRevB.74.214423 PACS number(s): 75.30.Kz, 75.47.Gk, 73.23.−b

I. INTRODUCTION

The discovery of "colossal magnetoresistance" (CMR) in 1994 reignited a lot of interest in hole-doped manganese oxides with the perovskite structure, also known as manganites.[1] In these materials, a complex interplay among the charge, spin, lattice, and orbital degrees of freedom has challenged our understanding of transition-metal oxides.[2,3] Zener linked the delocalization of the valence electrons with ferromagnetism through double exchange, which correlates charge and spin.[4] The coupling of charges with phonons and orbitals comes about through the Jahn-Teller effect, which tends to compete with the double exchange and localize carriers with a self-induced crystal distortion.[5,6] All of these competing interactions lead to a very rich and complex phase diagram, with a ferromagnetic metal (FMM) and a charge-ordered insulator (COI) being the two most relevant phases.[5]

Because of the near energetic degeneracy of various neighboring phases, magnetic and structural phase boundaries can be readily modified by external perturbations, which leads to many extraordinary properties with CMR as a specific example. There is compelling evidence, both experimental and theoretical, suggesting that in many cases the CMR effect occurs as a percolative process.[7] Quenched chemical disorder and an inhomogeneous distribution of strain result in the coexistence of FMM and COI phases with domain size as large as ~ 1 μm.[8,9] The magnetic field modifies the energetic balance between these competing phases and their phase fractions respond in kind. For example, as soon as the FMM phase fraction reaches the percolation threshold, the sample resistance plummets. Because of the vast resistivity contrast between FMM and COI phases, current transports through connected FMM domains, effectively forming conducting filaments.[10,11] Among various techniques of observing directly multiphase coexistence, magnetic force microscope images were used to correlate the percolation of FMM domains with the steep resistivity drop at the transition temperature.[10] Such conducting filaments were also observed by a magneto-optical imaging technique.[11] Besides magnetic field, other types of external perturbation, such as electric current or electromagnetic radiation, can also create conducting filaments.[12,13] Along the filaments, the connecting channels between the FM domains can be narrow.[14] Such weak links may make the conducting filaments fragile and sensitive to external perturbations. It is clear that many issues remain open regarding the morphology and dynamics of the conducting filaments and the interaction between them.[14]

Although the exact origin and nature of the phase coexistence remains an area of debate, there is consensus that submicrometer scale phase coexistence does exist in many manganite samples, both bulk and thin films. In these samples, however, conventional magnetic and transport measurements often render averaged results of the coexisting phases, smearing their individual contributions. Because of the percolative, filamentary nature of transport, mesoscopic structures with confined geometries are expected to differ from those of bulk and thin-film samples, which possess many more spatial degrees of freedom. The present work is an investigation of the impact of this scaling down the effective sample dimension into the mesoscopic (several hundreds of nanometers to several micrometers) regime, comparable to the domain size of the coexisting phases.

The material system we select is $Pr_{0.65}(Ca_{0.75}Sr_{0.25})_{0.35}MnO_3$ (PCSMO), a canonical system with multiphase coexistence.[15] In bulk PCSMO samples, it has been well established by neutron diffraction, magnetization, and electrical conductivity measurements that the COI and FMM phases coexist in a wide temperature range. A charge-ordering transition at ~ 220 K was followed on cooling by a sluggish first-order transition into FMM phase. Below T_C of 160 K, mesoscopic COI and FMM domains develop and coexist, which is also the focus of this report.

Here we report two sets of experiments focusing on the transport properties of PCSMO structures laterally confined to the mesoscopic scale. In the first set of experiments, a magnetic field triggers spontaneous jumps in resistance, but no clear anomaly is observed in the magnetization of the sample. These observations are consistent with the creation of conducting filaments without significant modification of the FMM phase fraction. Turning off the magnetic field annihilates the conducting filaments, which again produces discrete jumps in resistance. In the second set of experiments, we measure the current-voltage characteristics of the mesoscopic structures. As we reported previously,[16] in certain regimes of temperature and magnetic field, we observe a sharp, steplike decrease of current, or negative differential resistance (NDR), at critical bias voltages. The effect of tuning external parameters on this phenomenon indicates strong correlation with phase separation and filamentary transport. We propose that the origin of this effect is annihilation of individual conducting filaments by local Joule heating, which transforms local FMM regions to COI. These sets of experiments, then, demonstrate two complementary aspects of transport in a patterned structure of mixed phase manganites: magnetic field creates new conduction pathways leading in a stepwise way to enhanced conductivity; current destroys these pathways, abruptly reducing the current carried by the FMM filaments. A device length scale comparable to that of the phase-segregated components is essential to observing these complementary transport phenomena.

II. EXPERIMENTS

Epitaxial 800-Å thin films of $Pr_{0.65}(Ca_{0.75}Sr_{0.25})_{0.35}MnO_3$ were grown on $SrTiO_3$ (STO) substrates by pulsed laser deposition. Detailed deposition conditions and structural characterizations have been reported previously.[17,18] The substrates were held at constant temperatures between 700 and 800 °C under an oxygen pressure of 400 mTorr. After deposition, the samples were slowly cooled to room temperature in an environment of ambient oxygen. X-ray diffraction data shows that all films are (001) oriented with a small tensile strain of ~0.5%. The morphology of the films and the fabricated structures was imaged by a Dimension 3000 atomic force microscope (AFM) from Digital Instruments. Magnetization measurements were performed on a Quantum Design superconducting quantum interference device (SQUID) magnetometer. For transport measurements, we used a Quantum Design physical properties measurement system (PPMS) locally modified to measure high resistance. The current-voltage characteristics were measured with a Keithley 6487 picoammeter/voltage source. Submicrometer structures of PCSMO were patterned using electron-beam lithography. Since the ion-milling rate of manganite films is even smaller than that of the e-beam resist, patterned samples were etched 20 s in a diluted HCl solution prior to ion milling. Such a combination of chemical etching and ion milling allows reproducible submicrometer patterning without any significant damage from the Ar ions.

III. ANOMALOUS MAGNETORESISTANCE AND SLOW RELAXATION

It is relevant to explore how these films behave vis-à-vis their bulk analogs. In particular, we wish to establish that

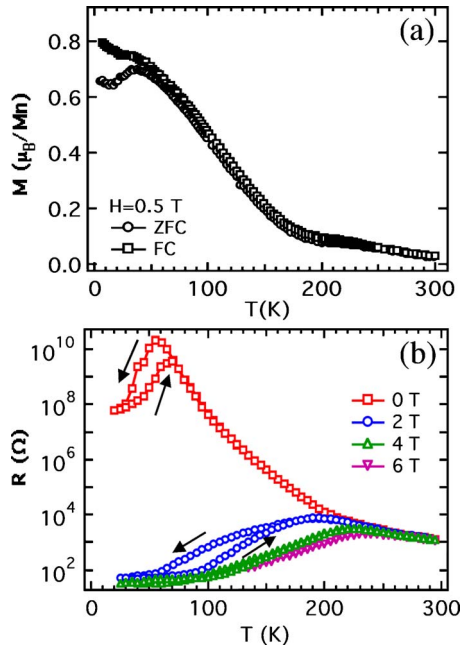

FIG. 1. (Color online) (a) ZFC and FC magnetization vs temperature curves measured in an applied field of 0.5 T for an 800-Å PCSMO film. (b) Plots of resistance vs temperature measured under various magnetic fields for the same film. Arrows indicate the directions of cooling and warming.

FMM and COI phases coexist in these films over a substantial temperature and magnetic field range. Magnetization and transport data demonstrate that this is, indeed, the case. Figure 1(a) shows the zero-field cooled (ZFC) and the field cooled (FC) magnetization vs temperature curves measured in an applied field of 0.5 T for an 800-Å PCSMO film. The small feature near 220 K is a signature of the CO transition, in agreement with the bulk behavior.[15] Below the CO temperature, magnetization shows an upturn, corresponding to increase of the FM phase. The FC curve continues to increase with decreasing temperature. However, the FM phase fraction remains below 20%, as indicated by the low-temperature magnetization of only ~0.8 μ_B/Mn. The ZFC curve peaks at ~35 K, below which the two curves depart from one another.

Plots of resistance vs temperature measured under various magnetic fields are shown in Fig. 1(b). All curves show resistive peaks, which are most likely percolative transitions instead of homogeneous insulator-metal transitions. The transport properties of the sample are dramatically modified by the magnetic fields. A field of 2 T increases the resistive peak temperature by ~150 K. The resulting magnetoresistance (MR) is colossal and is on the order of 10^8. The high MR suggests that the ratio of resistivity between COI and FMM phases must be larger than 10^8 at low temperatures since the material is a mixture of two phases both before and after the transition. All curves, especially those under lower magnetic fields, show substantial thermal hysteresis, which is characteristic of manganites with the FMM and COI phases competing in the vicinity of a first-order phase transition.

The AFM images of two typical structures, a 0.9 μm $\times$9.2 μm bridge and a 1.2 μm$\times$6 μm "S"-shaped structure

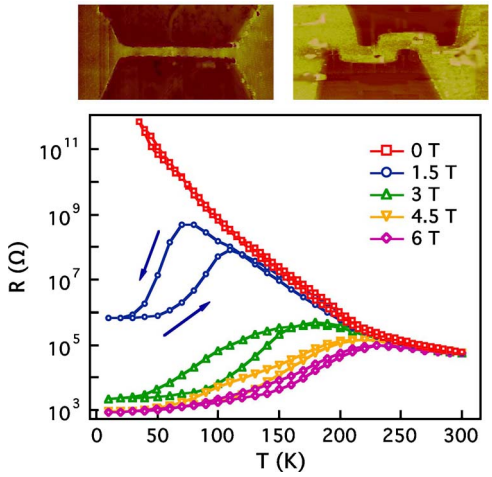

FIG. 2. (Color online) $R(T)$ under various magnetic fields data for the sample with a shape of narrow bridge. As an example, for the 1.5-T curve, the arrows specify the directions of cooling and warming. In general, the cooling curve shows higher resistance than the warming curve. Also shown are the AFM images of two typical structures, a 0.9 μm$\times$9.2 μm bridge and a 1.2 μm$\times$6 μm "S"-shaped structure.

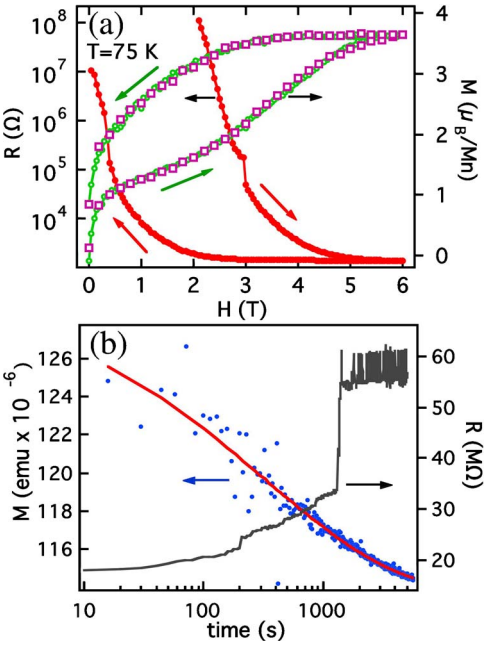

FIG. 3. (Color online) (a) Resistance vs magnetic field curves measured after ZFC to 75 K. Also shown are two magnetization vs magnetic field curves measured with different field steps (2000 Oe and 500 Oe, respectively) and average ramping (measurement) speeds (~10 Oe/s and ~3 Oe/s, respectively), demonstrating the reproducibility of the data. The increase and decrease of the magnetic field are indicated by arrows. (b) Relaxation of magnetization and resistance after the magnetic field cycle as described in text. The magnet charging speed is 200 Oe/s during the magnetic field cycle. The time dependence of the magnetization is fitted to the stretched exponential form shown as the solid line.

are shown in Fig. 2. Figure 2 shows $R(T)$ data for the narrow bridge. Qualitatively similar transport behaviors were found for the "S"-shaped structure. First, without magnetic field no peak is found down to the lowest temperatures for which we could measure a resistance. We believe that this is a natural consequence of the mesoscopic confinement. A single micrometer-scale COI domain can in principle block the current flow in this narrow constriction, while many alternative paths exist in film and bulk samples. Alternatively, it is also possible that an extrinsic defect could cause such an insulating behavior, amplified by the confined geometry. However, under a magnetic field of 1.5 T, a resistance peak appears at 75 and 115 K on cooling and warming, respectively. It is unlikely that an extrinsic defect in the film would respond to magnetic fields. Furthermore, increasing the field moves the resistance peaks to even higher temperatures. At low temperatures, a magnetic field of 6 T reduces the sample resistance to 1000 Ω. Ignoring contact resistance, the resistivity of the film is estimated to be smaller than 1 mΩ cm at 25 K, indicating a high fraction of the FMM phase under these conditions. By analogy to bulk materials, we argue that this demonstrates a FMM phase fraction large enough to percolate through the structure. These characteristics are qualitatively reproduced in all mesoscopic structures. The combined transport and magnetization data are qualitatively similar to those found in bulk samples of PCSMO. In addition, the behavior parallels that found by Zhang *et al.* for films of $La_{0.33}Pr_{0.34}Ca_{0.33}MnO_3$ in which FMM/COI phase coexistence has been established by magnetic force microscopy studies.[10]

We now turn to a more detailed examination of the magnetotransport characteristics of these structures. Figure 3(a) shows the MR and $M(H)$ curves measured on the same sample. The resistance is too high to measure on the increasing branch when the field is below 2 T. The high resistance suggests that the FMM domains are separated or poorly connected. This assertion is corroborated by the $M(H)$ curve. A plateau at ~1 T corresponds to full alignment of the regions which are ferromagnetic at zero field,[19] but a higher field is required to transform COI phase to FMM, as indicated by the metamagnetic transition at ~1.8 T. Both resistance and magnetization curves show significant hysteresis, hallmarks of the magnetic field-induced conversion of COI to FMM phase. The most significant feature is that the MR data of mesoscopic structures at 75 K where FMM and COI coexist exhibit anomalous behaviors. Both branches of MR curves produced by increasing and decreasing H are interrupted by spontaneous jumps. The onset of these resistive jumps shows no apparent dependence on the measurement protocols such as field step size and ramping speed. Unlike the MR curves, $M(H)$ curves measured at difference field step sizes and speeds do not show the steplike jumps above experimental noise. Therefore, it is unlikely that these resistive jumps are a result of homogeneous magnetic transitions. Rather, we suggest that small, localized regions in the bridge become electrically connected by the FMM phase at these jumps. At these jumps, either some COI phase is converted to FMM or the morphology of the FMM phase changes without an increase in phase fraction. If the former, then the steplike higher magnetization resulting from the conversion of these regions is apparently too small to measure in the SQUID

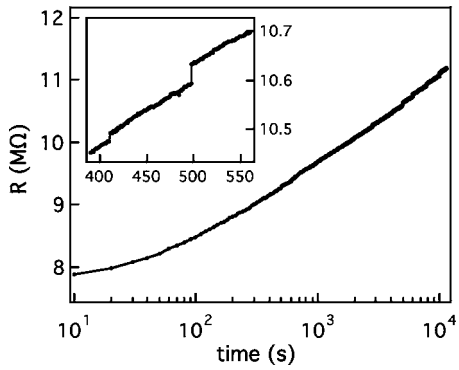

FIG. 4. Resistive relaxation after the magnetic field cycle measured on a continuous film. The inset is an amplified view.

magnetometer. We suggest that the jumps in the MR curves originate from the magnetic-field-induced creation and annihilation of single or a few conducting filaments. These negligible modifications of the FMM phase fraction are amplified and exhibit steplike features in the MR measurements.

We have also examined the time-dependent magnetic and transport properties of the samples. The sample is ZFC to 75 K. Then the magnetic field is ramped to 6 T with a speed of 200 Oe/s where the sample is kept for 10 min and we start measurements after ramping the field back to zero with the same speed. Shown in Fig. 3(b), at 75 K the slow increase (decrease) of the resistance (magnetization) after the field cycle is consistent with a decreasing FMM phase fraction. The most notable feature is the sudden jumps in $R(t)$ sporadically distributed over the waiting period of 1.5 h. Several runs for different samples all exhibit such jumps, although the exact time of the jumps is not reproducible. The absence of any apparent singularity in the magnetization measurement agrees with the behavior seen in the $M(H)$ curves. Similar relaxation effects were observed in a $Pr_{0.67}Ca_{0.33}MnO_3$ single crystal, which has been interpreted as the suppression of the metallic paths below the percolation threshold.[20]

There are two additional features during relaxation worth mentioning briefly. First, after the resistive jumps we frequently observe a two-level switching behavior whose amplitude is ~10% in Fig. 3(b). Such a switching behavior has been noted in $La_{5/8-y}Pr_yCa_{3/8}MnO_3$ and $La_{2/3}Ca_{1/3}MnO_3$, where it was linked to the concerted fluctuation between the FMM and a less conducting phase.[21,22] Second, the relaxation of magnetization obeys reasonably well the stretched exponential form $M(t)=M_0-M_1\ \exp[-(t/\tau)^\beta]$ with $\beta\sim0.4$ and $\tau\sim325$ s. This form was used previously to characterize the time decay of the remanent magnetization in a spin glass.[23] It was proposed that the slow dynamics of the FMM domain boundaries could lead to such a spin-glass-like behavior.[24]

Since it is a result of inhomogeneous, filamentary conduction, the occurrence of the spontaneous resistive jumps is not expected to depend on sample size. However, the characteristics of the steps may. Figure 4 demonstrates the relaxation behavior of a continuous film with the same composition and thickness as the mesoscopic structures. The effective area measured is about 5 mm long and 1 mm wide. Although invisible on the large scale of the main panel, small resistive jumps do exist, as can be seen in the inset. Compared to mesoscopic structures, the magnitude of the steps is reduced by almost 10^3. However, we need to note here that the spontaneous giant resistive jumps and/or slow relaxation have also been observed in bulk samples of manganites with other compositions.[19,20,25,26] The characteristics of these anomalous transport behaviors depend on the sample composition, degree of disorder, ramping speed of external magnetic field, etc. In some of the previous studies, the spontaneous resistive jumps were contributed to the conversion of atomic clusters, which may not form conducting filaments as in our samples. Nevertheless, our experimental data reported here is consistent with the mesoscopic phase separation and filamentary conduction observed in PCSMO and manganites with other similar compositions.[10,11,15]

It remains an open question whether the spontaneous resistive jumps observed in the MR and relaxation measurements are a result of modified FMM phase fraction or a morphological change of the FMM domains. Concerning the latter scenario, small linking FMM clusters and larger domains could merge together under stress from the surrounding phase.[27] Such a morphological modification of the conducting filaments could also lead to large resistive jumps. Both scenarios require little or no change of magnetization, consistent with the experimental observation. Tools capable of observing magnetic domains directly are required to distinguish these two scenarios.

IV. NEGATIVE DIFFERENTIAL RESISTANCE DUE TO ANNIHILATION OF CONDUCTING FILAMENTS

Recently, it was demonstrated that electric field and current also have colossal effects on the transport properties of manganites, comparable to CMR.[11,12,28] Such voltage and current effects are usually ignored in MR measurements with constant bias. In Fig. 5, current vs voltage (I-V) curves were taken on the "S"-shaped PCSMO structure at six temperatures from 100 to 225 K. At 100 K and for $H<2$ T, the I-V curves are ohmic. At 2 T, the I-V curve becomes convex as the voltage increases. Similar current-induced nonlinear conductions observed in $Pr_{0.5}Ca_{0.5}MnO_3$ thin films were suggested to be a result of Joule heating.[29] The most salient feature of the I-V curve is a steplike decrease in current, or NDR, at a threshold voltage (V_{C1}) of ~37 V. V_{C1} decreases systematically with increasing magnetic field. At and above 2.4 T, a second threshold voltage, V_{C2}, emerges, which also systematically moves to lower voltage with increasing magnetic field. These NDR steps are quite sharp at 100 K and the I-V curves exhibit slight hysteresis at the steps upon reducing the bias voltage. A typical loop taken at a field of 2.8 T is shown in the inset of Fig. 8, where the threshold voltage is slightly lower as the voltage ramps back to zero. Consecutive ramping up of voltage results in the same curve within the measurement error.

The I-V curves taken at 100 K on the narrow bridge sample with the same composition of PCSMO are shown in Fig. 6. Qualitatively similar NDR behaviors are found on both types of samples ("S"-shaped structures and narrow

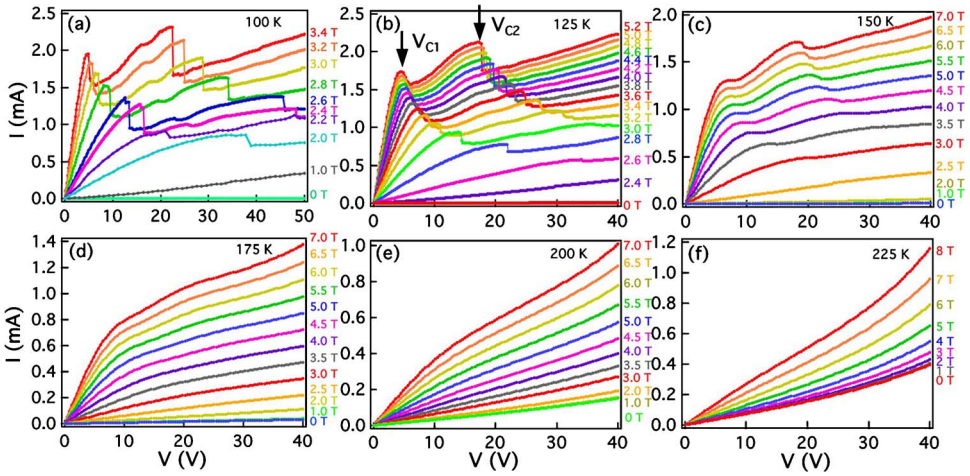

FIG. 5. (Color online) Current vs voltage curves of the "S"-shaped PCSMO structure measured in various magnetic fields at 100 (a), 125 (b), 150 (c), 175 (d), 200 (e), and 225 (f) K. The voltage sweep rate is ~0.5 V/s. As an example, arrows identify critical voltages, V_{C1} and V_{C2}, on the 125 K, 5.2 T curve.

bridges) although the exact values of the critical magnetic field and the threshold voltages to trigger NDR are different. Therefore, the anomalous behavior observed in the *I-V* curves is a common feature for the mesoscopic PCSMO structures. In the following analysis and discussion, we will focus on the data taken on the "S"-shaped structure.

The NDR steps have a *T* dependence that can be correlated with the FMM/COI mixed phase characteristics of the PCSMO composition. At 125 K, NDR steps appear under magnetic fields $\geqslant$2.8 T; a precursor feature can be seen at 2.6 T. Their magnitude is smaller than that at 100 K. Both of these temperatures are deep in the region with phase coexistence, as shown by the hysteretic behavior in Fig. 2. At 150 K, the NDR steps are smoothed but still persist. At 175 K, which approaches the edge of the hysteresis region, no NDR features are observed under conditions accessible to our experiment, except some remnant features at the voltages where NDR steps occur at lower temperatures. The convex curvature of the *I-V* curves persists at 200 K but totally disappears at 225 K, which lies outside of the hysteresis region of the RT curves. This temperature dependence strongly suggests that phase separation is indispensable for the onset of these NDR steps.

Similar NDR was observed in vanadium dioxide at its Néel temperature of 68 °C.[30] This transition from a low-*T* monoclinic semiconductor to a high-*T* tetragonal metal has a first-order displacive nature.[31] VO_2 and our PCSMO samples share the following common characteristics: (i) their transitions are first order, involving two phases with different structural, magnetic, and electrical properties; (ii) near the phase transition temperature, two phases coexist in both materials; (iii) due to the conductivity contrast between the phases, the current distribution is inhomogeneous and concentrates in low-resistivity filaments. In VO_2, NDR is produced by a thermally induced resistive switching of the conducting filaments.[32,33] In the following, we argue that a similar Joule heating-assisted transition also triggers the anomalous *I-V* characteristics in our samples. In this scenario, as the bias voltage, or equivalently, the injected thermal power, reaches a critical value, a local Joule heating process assists one or a few conducting filaments to transform from the FMM phase to another phase with much higher resistance, presumably the competing COI phase. The annihilation of the conducting filament leads to the observed sudden decreases of current, or NDR. The small hysteresis shown in the inset of Fig. 8 is consistent with the first-order nature of the conversion between the phases.

To substantiate the hypothesis of heating-induced annihilation of conducting pathways, we analyze the *I-V* data using a straightforward resistor-network model. Due to the notorious difficulty associated with the theoretical estimation of resistivity, random resistor network models have been adapted to simulate the conduction in phase-separated manganites.[34] Such a network could possess complex configurations, even with a coarse-grain approximation. In our case, however, because the sample size is comparable to the dimension of FMM filaments, we use a considerably simplified, strictly phenomenological model built up of three parallel resistors. The model is schematically shown in the inset of Fig. 7(a). R_1 and R_2 represent "weak-link" resistors (conducting filaments composed of connected ferromagnetic metallic domains) that undergo an abrupt transition as *V* is increased. R_3 is taken collectively to represent all remaining conductive pathways that do not undergo a resistive transition in the bias voltage region we can access experimentally. A load resistor, R_L, represents all contributions from external resistance sources (contacts, leads, etc.). Below the threshold voltage V_{C1}, the overall resistance of the system is the parallel combination of R_1, R_2, and R_3 (ignoring for the moment R_L). At V_{C1}, R_1 abruptly becomes far more resistive (considered to be infinite in this analysis, a simplifying assumption that does not obscure the physics of the problem), and the

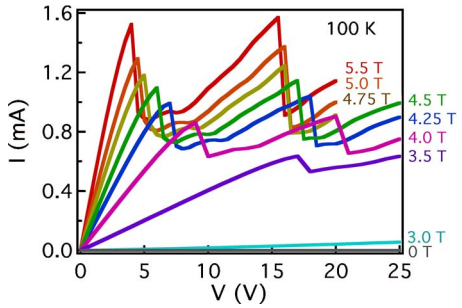

FIG. 6. (Color online) Current vs voltage curves of the PCSMO narrow bridge structure measured in various magnetic fields at 100 K. The voltage sweep rate is ~0.5 V/s.

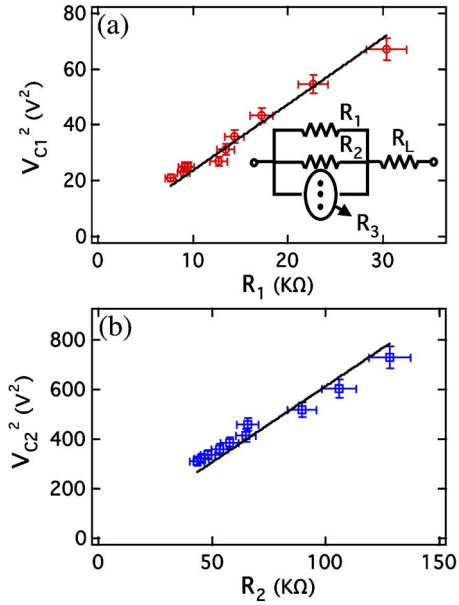

FIG. 7. (Color online) Filamentary conduction in the manganite structure is modeled as a network of parallel resistors as shown in the inset. (a) and (b) plot the square of the critical voltages vs the corresponding calculated values of R_1 and R_2 from the magnetic-field-dependent I-V curves taken at 125 K. Note that our proposed model suggests that the linear fit lines should go through the origin.

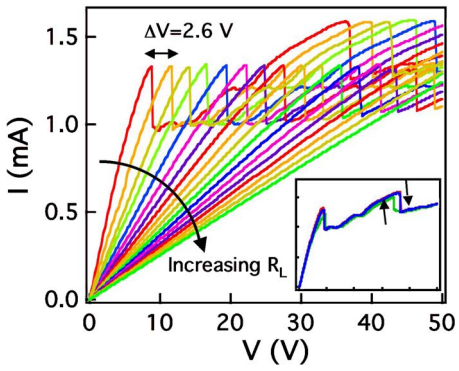

FIG. 8. (Color online) Series of I-V curves measured at 100 K and 2.8 T with R_L varying between 0 and 34 KΩ with a step of 2 KΩ. The arrow indicates the direction of increasing R_L. The inset shows a complete hysteresis loop without any load resistance. The units of the inset are the same as the main figure. The arrows indicate the field ramping directions. Also shown are I-V curves of two subsequent runs under the same conditions. Their overlapping with each other demonstrates the reproducibility of the switching.

network reduces to a simpler parallel combination of R_2 and R_3. Similarly, at V_{C2}, R_2 becomes infinite, redistributing current through R_3.

While this phenomenological model clearly simplifies the microscopic physics of the system, no additional complexity needs to be added to explain the I-V data. Specifically, the model (i) shows that the current (resistance) should decrease (increase) abruptly after each step and (ii) explains why a constant power input is found for the steps as magnetic field is varied. This latter observation is an essential consequence of the proposed resistor network scheme. Point (i) is easily seen to result from the progressive removal of conductive pathways at the critical voltages. The loss of such pathways at each step must lead to an increase in the total resistance of the network. Point (ii) can be seen by extracting magnetic-field-dependent values of R_1 and R_2 at the threshold voltages and computing the power injected into each filament. For example, for the case of 125 K and 5.2 T, shown as the top I-V curve in Fig. 5(b), the resistance values of the total network before $(R_1 \| R_2 \| R_3)$ and after $(R_2 \| R_3)$ the first NDR step are 2.5 KΩ and 3.8 KΩ, respectively. Then R_1 is calculated to be 7.3 KΩ. Similarly R_2 is calculated to be 43.4 KΩ using the resistance values across the second NDR step. Using this procedure, at the base temperature of 125 K, the values of R_1 and R_2 are extracted for each magnetic field. If the transitions are indeed thermally driven, then we would expect that they should occur at well-defined input power thresholds. These threshold power values occur when the net energy input (i.e., power delivered to the device minus thermal losses to substrate, contact, etc.) is sufficient to surmount the energy barrier between FMM and COI phases in some localized area of the filaments, phenomenologically labeled as R_i with $i=1,2$. At this point, the local region will convert from FMM to COI phase, effectively shutting off conduction in this path (i.e., $R_i \rightarrow$ infinity). The power delivered to a resistor is simply given by $P_i = V_{C1}^2 / R_i$. Therefore, if V_{C1}^2 vs R_1 is linear, the slope indicates a specific power value delivered to R_1 at V_{C1} (and likewise into R_2 at V_{C2}). Indeed, in Fig. 7(a), V_{C1}^2 vs R_1 is well fit by a straight line, from which $P_1 \sim 0.16 \pm 0.02$ mW. Similarly, Fig. 7(b) yields 0.42 ± 0.05 mW for P_2. Naturally, it is expected that these values will be sensitive to sample details, substrate properties, and other extrinsic effects. Thus, no particular quantitative significance should be attached to them. However, the observed linear relationship between R_i and V_{C1}^2 is a necessary consequence for the model proposed above. We note that the process of heat injection and dissipation is highly inhomogeneous as a result of the filamentary conduction. Therefore this process of inhomogeneous heat exchange and the final local temperatures in the system are challenging to analyze quantitatively.

This phenomenological model is in an extremely simple form and other models with a more complex network configuration may be also consistent with the experimental data. Indeed, R_L can be added in series to simulate the contact resistance or other sources of parasitic resistance. We find that $R_L \sim 400$ Ω improves our fits slightly, but such an arbitrary modification adds no physical insight.

Our assumption of constant critical powers at the steps also corresponds to constant critical current, which does not depend on the load resistance. To verify this, we add in series a variable resistor to systematically change the value of R_L from 0 to 34 KΩ with a step of 2 KΩ. Figure 8 shows the I-V curves modulated by R_L, taken at 100 K and under 2.8 T. Indeed, regardless of the value of R_L, the first and second steps always occur at 1.33 mA and 1.59 mA, respectively. The constant spacing of 2.6 V between the first critical voltages is a result of the incremental load resistance. Eventually, a load resistance of 32 KΩ eliminates the steps in the voltage range measured. This systematic displacement of I-V curves

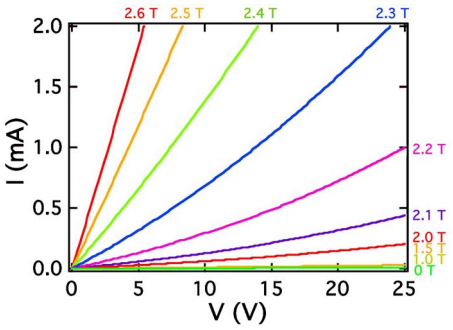

FIG. 9. (Color online) *I-V* curves taken at 125 K under various magnetic fields for a continuous PCSMO film. The voltage sweep rate is ~0.5 V/s.

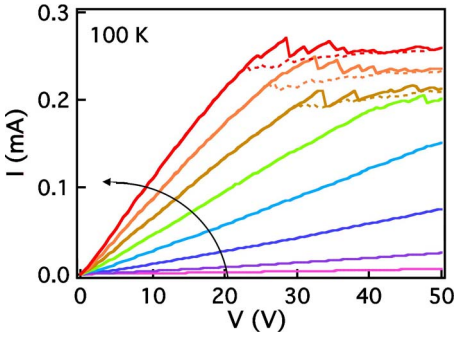

FIG. 10. (Color online) *I-V* curves taken at 100 K for a 0.9 μm×5.2 μm bridge with the composition of $La_{0.7}Ca_{0.3}MnO_3$. The solid (dashed) lines are the *I-V* curves taken with increasing (decreasing) voltages. The voltage sweep rate is ~0.5 V/s. The arrow indicates the magnetic field increased from 0 to 7 T with a step of 1 T.

also sheds light on the absence of steplike features in the continuous film shown in Fig. 9. The macroscopic dimension of the continuous film is accompanied by a much more complex equivalent resistor network. Since the total power is distributed over many more degrees of freedom, the Joule heating on individual resistors (filaments) is much reduced and not enough to trigger a NDR transition.

Finally, the phenomenology of the NDR steps and their dependence on the magnetic field and temperature should be dramatically modified in manganites with different chemical compositions. Both the fraction and the domain morphology of the ferromagnetic phase, and therefore the conducting filaments if they exist, can be tuned systematically by composition. Our preliminary results indicate that the mesoscopic structures of $La_{0.7}Sr_{0.3}MnO_3$ do not have any NDR steps in their *I-V* curves, presumably a result of the absence of a strong multiphase coexistence. We also fabricated narrow bridges of another canonical manganite, $La_{0.7}Ca_{0.3}MnO_3$ (LCMO). The magnetization and transport measurements done on continuous LCMO films show a T_C of ~200 K, lower than the bulk value of 250 K,[35] consistent with previous studies on strained LCMO films.[36] The $R(T)$ curves of the mesoscopic bridge structures (not shown here), however, show much reduced resistive peak temperatures of ~88 K and substantial thermal hysteresis, suggesting the significant effect of the sample sizes on the transport properties. In Fig. 10, we show the magnetic-field-dependent *I-V* curves taken at 100 K on a 0.9 μm×5.2 μm bridge of LCMO. After certain critical voltages, the *I-V* curves show numerous switching steps with sizes much smaller than those observed in the PCSMO samples. Voltage cycles result in significant hysteresis. Although the exact origin of these complex behaviors in $La_{0.7}Ca_{0.3}MnO_3$ remains unclear at this stage, they are likely to result from the response of the connected conducting domains to the external magnetic field and the injected thermal power, which is similar to the PCSMO samples.

V. CONCLUSIONS

In summary, steplike resistive transitions are observed in mesoscopic manganite structures. These steps are triggered by either magnetic or electric field. Specifically, the MR curves exhibit spontaneous jumps, which were also observed during resistive relaxation after magnetic field cycles. The absence of corresponding singularities in the magnetization measurements suggests that the conduction is not homogeneous but filamentary. Such resistive steps also exist in continuous films. However, their magnitude is dramatically reduced due to the averaging effect over a much higher number of filaments. In the same samples, by tuning temperature and external magnetic field we also observed steplike NDR at critical voltages. We explain these observations as a heating effect that effectively annihilates the conduction along a specific conducting filament by locally converting an FMM region to COI as the injected power reaches critical values. Under the same experimental conditions, NDR does not exist in continuous films due to the much lower heating power distributed into individual filaments. Both magnetic and electric fields have been shown to affect the creation and annihilation of conducting filaments in maganites with multiphase coexistence, but through different routes. The magnetic field always favors the growth of FMM phase over other phases, effectively creating filamentary conducting paths. On the other hand, the electric field or current-triggered effects on manganites has different origins. In the present case, the observed anomalies in the *I-V* curves are not directly induced by the bias voltage or current, but rather by Joule heating.

It is still under debate whether the widely observed phase separation originates from intrinsic or extrinsic factors. Strong phase separation is often observed in samples with pronounced chemical or structural disorder and inhomogeneities. However, even single crystals exhibit such a coexistence of multiple phases, although they are free from any perceptible impurities or substrate stress.[11,37] Furthermore, the disorder does not fix the domain pattern or pin the movement of domain boundaries.[11] In our experiments, the mesoscopic confinement may modify the morphology and dynamics of the filamentary domains. The fact that we have found similar transport behavior in structures with different shapes argues for an intrinsic nature to the observed phenomenon. It is unlikely that spin-dependent scattering across some extrinsic chemical and structural impurities alone could produce all the systematic dependence of the data on the temperature and magnetic field. In fact, defects accidentally created dur-

ing sample fabrication, such as uneven boundaries and large particulates, destroy the steplike resistive transition. These defect samples also show little MR effect, probably a result of excessive pinning of domain walls. Even though intrinsic in many cases, multiphase coexistence and the ensuing formation of conducting filaments do not necessarily represent the true equilibrium state of the system. Strong relaxation of resistance and dependence on magnetic history observed in both our samples and others suggests a metastable state with a spin-glass-type hierarchical energetic landscape.[38] Even nanosized manganese clusters could switch between different phases, giving rise to giant random telegraph noise.[39]

For the compositions studied here, the presented dramatic modification of transport properties results directly from the mesoscopic dimension of the samples. It may have important implications for scaling down other similar materials with phase coexistence. Currently, we are studying structures with different dimensions to explore systematically the effect of confinement. There are several questions left unanswered: what is the largest dimension for the sample to retain its anomalous transport properties? After being scaled down farther, will the sample remain phase-separated or become single phase? What are the effects of film thickness and chemical composition? Our preliminary results suggest that for this specific manganite composition of $Pr_{0.65}(Ca_{0.75}Sr_{0.25})_{0.35}MnO_3$, the NDR feature exists only in devices with dimensions of a few micrometers or smaller. However, more systematic studies on the dimension and composition dependence are needed to achieve better understandings of these anomalous transport properties. Finally, it is crucial to observe the change of the filamentary conducting paths using direct tools with submicrometer spatial resolution, such as magneto-optical imaging techniques, magnetic force, or electron microscopy.[10,11,40]

Note added in proof. Recently, we became aware of the work by Zhai *et al.*[41] Their observation and interpretation of giant discrete resistance steps in laterally patterned structures of manganite with phase coexistence are consistent with the findings reported here.

ACKNOWLEDGMENTS

Argonne National Laboratory Center for Nanoscale Materials work was supported by the U.S. Department of Energy, Office of Science, Office of Basic Energy Sciences, under Contract No.W-31-109-ENG-38. We also acknowledge helpful discussions with D. I. Khomskii, A. Hoffmann, and M. Tokunaga.

*Present address: Division of Physics and Applied Physics, School of Physical and Mathematical Sciences, Nanyang Technological University, 1 Nanyang Walk, Singapore 637616. Email address: tomwu@ntu.edu.sg

[1] S. Jin, T. H. Tiefel, M. McCormack, R. A. Fastnacht, R. Ramesh, and L. H. Chen, Science **264**, 413 (1994).
[2] C. N. R. Rao and B. Raveau, in *Colossal Magnetoresistance, Charge Ordering, and Related Properties of Manganese Oxides*, edited by C. N. R. Rao and B. Raveau (World Scientific, Singapore, 1998).
[3] Y. Tokura, in *Colossal Magnetoresistance Oxides*, edited by Y. Tokura (Gordon & Breach, London, 1999).
[4] C. Zener, Phys. Rev. **82**, 403 (1951).
[5] A. J. Millis, Nature (London) **392**, 147 (1998).
[6] Y. Tokura and N. Nagaosa, Science **288**, 462 (2000).
[7] E. Dagotto, T. Hotta, and A. Moreo, Phys. Rep. **344**, 1 (2001).
[8] J. Burgy, M. Mayr, V. Martin-Mayor, A. Moreo, and E. Dagotto, Phys. Rev. Lett. **87**, 277202 (2001).
[9] K. H. Ahn, T. Lookman, and A. R. Bishop, Nature (London) **428**, 401 (2004).
[10] Liuwan Zhang, Casey Israel, Amlan Biswas, R. L. Greene, and Alex de Lozanne, Science **298**, 805 (2002).
[11] M. Tokunaga, Y. Tokunaga, and T. Tamegai, Phys. Rev. Lett. **93**, 037203 (2004).
[12] A. Asamitsu, Y. Tomioka, H. Kuwahara, and Y. Tokura, Nature (London) **388**, 50 (1997).
[13] M. Fiebig, K. Miyano, Y. Tomioka, and Y. Tokura, Science **280**, 1925 (1998).
[14] J. H. Yoo, Y. Murakami, D. Shindo, T. Atou, and M. Kikuchi, Phys. Rev. Lett. **93**, 047204 (2004).
[15] G. R. Blake, L. Chapon, P. G. Radaelli, D. N. Argyriou, M. J. Gutmann, and J. F. Mitchell, Phys. Rev. B **66**, 144412 (2002).
[16] T. Wu and J. F. Mitchell, Appl. Phys. Lett. **86**, 252505 (2005).
[17] T. Wu and J. F. Mitchell, Phys. Rev. B **69**, 100405(R) (2004).
[18] T. Wu and J. F. Mitchell, J. Magn. Magn. Mater. **292**, 25 (2005).
[19] I. G. Deac, S. V. Diaz, B. G. Kim, S.-W. Cheong, and P. Schiffer, Phys. Rev. B **65**, 174426 (2002).
[20] A. Anane, J. P. Renard, L. Reversat, C. Dupas, P. Veillet, M. Viret, L. Pinsard, and A. Revcolevschi, Phys. Rev. B **59**, 77 (1999).
[21] R. D. Merithew, M. B. Weissman, F. M. Hess, P. Spradling, E. R. Nowak, J. O'Donnell, J. N. Eckstein, Y. Tokura, and Y. Tomioka, Phys. Rev. Lett. **84**, 3442 (2000).
[22] V. Podzorov, M. E. Gershenson, M. Uehara, and S. W. Cheong, Phys. Rev. B **64**, 115113 (2001).
[23] R. V. Chamberlin, George Mozurkewich, and R. Orbach, Phys. Rev. Lett. **52**, 867 (1984).
[24] M. Uehara and S. W. Cheong, Europhys. Lett. **52**, 674 (2000).
[25] M. Matsukawa, K. Akasaka, H. Noto, R. Suryanarayanan, S. Nimori, M. Apostu, A. Revcolevschi, and N. Kobayashi, Phys. Rev. B **72**, 064412 (2005).
[26] V. Markovich, G. Jung, Y. Yuzhelevski, G. Gorodetsky, A. Szewczyk, M. Gutowska, D. A. Shulyatev, and Y. M. Mukovskii, Phys. Rev. B **70**, 064414 (2004).
[27] J. Stankiewicz, J. Sese, J. Garcia, J. Blasco, and C. Rillo, Phys. Rev. B **61**, 11236 (2000).
[28] V. Ponnambalam, S. Parashar, A. R. Raju, and C. N. R. Rao, Appl. Phys. Lett. **74**, 206 (1999).
[29] P. Padhan, W. Prellier, Ch. Simon, and R. C. Budhani, Phys. Rev. B **70**, 134403 (2004).
[30] B. Fisher, J. Phys. C **8**, 2072 (1975).
[31] F. J. Morin, Phys. Rev. Lett. **3**, 34 (1959).
[32] J. Duchene, M. Terraillon, P. Pailly, and G. Adam, Appl. Phys.

Lett. **19**, 115 (1971).
[33] J. L. Jackson and M. P. Shaw, Appl. Phys. Lett. **25**, 666 (1974).
[34] M. Mayr, A. Moreo, J. A. Verges, J. Arispe, A. Feiguin, and E. Dagotto, Phys. Rev. Lett. **86**, 135 (2001).
[35] P. Schiffer, A. P. Ramirez, W. Bao, and S. W. Cheong, Phys. Rev. Lett. **75**, 3336 (1995).
[36] W. Prellier, A. Biswas, M. Rajeswari, T. Venkatesan, and R. L. Greene, Appl. Phys. Lett. **75**, 397 (1999).
[37] D. D. Sarma, D. Topwal, U. Manju, S. R. Krishnakumar, M. Bertolo, S. La Rosa, G. Cautero, T. Y. Koo, P. A. Sharma, S.-W. Cheong, and A. Fujimori, Phys. Rev. Lett. **93**, 097202 (2004).
[38] R. von Helmolt, J. Wecker, L. Lorenz, and K. Samwer, Appl. Phys. Lett. **67**, 2093 (1995).
[39] B. Raquet, A. Anane, S. Wirth, P. Xiong, and S. von Molnar, Phys. Rev. Lett. **84**, 4485 (2000).
[40] Y. Murakami, J. H. Yoo, D. Shindo, T. Atou, and M. Kikuchi, Nature (London) **423**, 965 (2003).
[41] Hong-Ying Zhai, J. X. Ma, D. T. Gillaspie, X. G. Zhang, T. Z. Ward, E. W. Plummer, and J. Shen, Phys. Rev. Lett. **97**, 167201 (2006).